Nanodevices in Flatland: Two-dimensional graphene-based transistors with high I_{on}/I_{off} ratio

G.Fiori, A. Betti, S. Bruzzone, P. D'Amico, G. Iannaccone
Dipartimento di Ingegneria dell'Informazione
Università di Pisa, Via Caruso I-56122 Pisa, Italy
Tel. +39 050 2217639; Fax. +39 050 2217522, email: gfiori@mercurio.iet.unipi.it

***Abstract*— We present a multi-scale investigation of graphene-based transistors with a hexagonal boron-carbon-nitride (h-BCN) barrier in the channel. Our approach exploits ab-initio calculations for an accurate extraction of energy bands and tight-binding simulations in order to compute charge transport. We show that the h-BCN barrier inhibits the ambipolar behavior of graphene transistors, leading to a large I_{on}/I_{off} ratio, within the ITRS roadmap specifications for future semiconductor technology nodes.**

I. Introduction

We present a new platform for the exploration of graphene-based two-dimensional devices, characterized by engineering of hybridized graphene. Recent experiments [1] have shown the possibility of fabricating two-dimensional hybrid structures consisting of intercalated carbon and h-BCN (hexagonal boron carbon nitrogen) domains. Electronic and mechanical properties of such domains can be tuned by varying the relative fractions of the three elements, which in turn depend on pressure, temperature, and gas concentration during the thermal catalytic CVD growth.

We believe this can open new routes for graphene nanoelectronics, because hybrid h-BCN-graphene structures provide the opportunity to overcome intrinsic limitations of "pure" graphene: the zero bandgap and the fully ambipolar behavior [2], [3].

Graphene has a zero bandgap, but - as we show - h-BCN domains can have a gap between 1 and 5 eV. Proper use of h-BCN domains can allow to suppress the ambipolar behavior, blocking flow of one type of carriers, and to fully modulate current due to carriers of the other type.

The basic device is illustrated in Fig. 1. It is a double-gate FET with a band-engineered channel, including an h-BCN region below the gate, acting as the real barrier for carrier flow, and two graphene leads towards the source and drain contacts. Graphene regions below the gate are undoped, whereas the rest is doped with donors or acceptors for obtaining nFETs or pFETs, respectively.

Here, we explore the possibility offered by hybrid h-BCN-graphene structures for truly planar nanoscale devices, using a multiscale simulation approach coupling ab-initio simulations based on density-functional theory (DFT) with quantum transport device simulations based on the Non-equilibrium Green's functions (NEGF) formalism and on an atomistic tight-binding (TB) Hamiltonian.

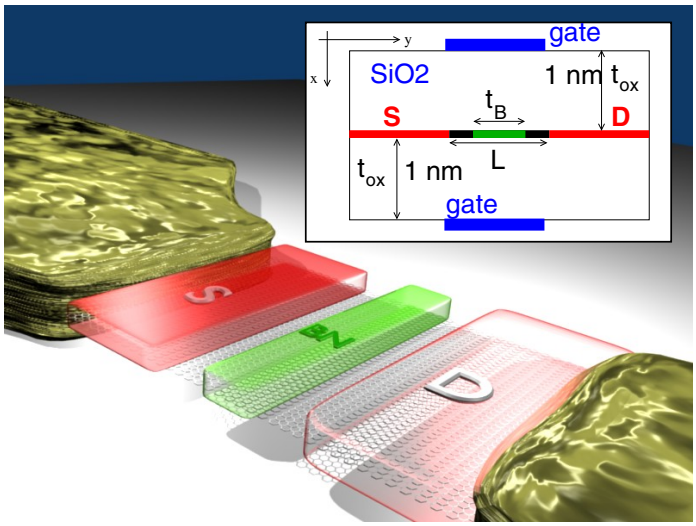

Fig. 1. Graphene-based transistor with BN barrier in the channel (top and bottom gates are not depicted). In the inset, a longitudinal cross-section of the device is shown. Top and bottom oxides thickness $t_{ox} = 1$ nm. Source and drain reservoirs are 10-nm long with a molar fraction f. t_B is the barrier thickness, and L is the channel length.

II. Methodology

DFT calculations have been performed by means of the Quantum ESPRESSO code [4] using a plane wave basis set in the generalized gradient approximation (GGA) with the Perdew-Burke-Ernzerhof (PBE) exchange correlation functional.

We have considered a 65 Ry wave function cutoff and 400 Ry charge density cutoff. The Brillouin zone has been sampled using a 30×30×2 Monkhorst-Pack grid. A 30 bohr layer of vacuum separates the sheet from its periodical images, which is sufficient to avoid any unphysical interactions.

The geometries are fully relaxed without any symmetry constraints, while the convergence of total energy and force are set to 1×10^{7} a.u.

We have computed energy dispersion relations, from which we have extracted tight-binding parameters, in order to be able to accurately reproduce the bottom conduction band and the top valence band. We used the tight binding parameters in our open-source device simulation package NanoTCAD ViDES [5], to evaluate device operation through the self-consistent solution of the 2D Poisson and the Schroedinger equation with open boundary conditions, within the Non-Equilibrium Green's Function (NEGF) formalism.

In particular, we have described the Hamiltonian for the

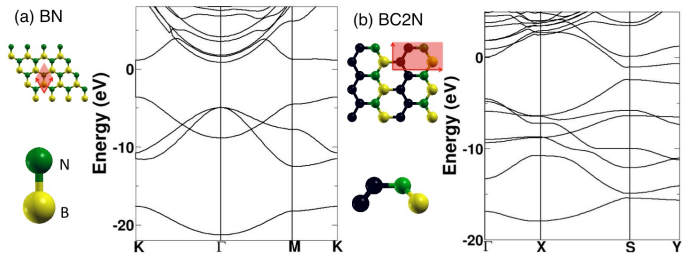

Fig. 2. h-BCN materials. For each material, the primitive cell and the bands computed by means of DFT-GGA simulations are shown.

considered two-dimensional material taking into account Bloch periodic boundary conditions along the transversal direction with period $\Delta = 3a_{cc}$, where a_{cc} = 0.144 nm is the carbon-carbon bonding distance [6], [7], which leads to a k_x wave vector dependence in the Hamiltonian, Semi-infinite contacts have been modeled along the longitudinal direction by means of self-energies.

The extracted tight-binding parameters for the BN are in good agreement with recently published results [8].

In order to improve the speed of the overall procedure, an efficient algorithm for a fast computation of the self-energies has been exploited [9] and included in the NanoTCAD ViDES framework. In particular, the adopted algorithm computes the self-energy by means of a closed-form procedure, which is at least 20 times faster than other iterative methods [10].

III. Results and Discussion

The device structure is shown in Fig. 1: the channel is embedded in SiO_2, the thickness of the top and bottom field oxides is 1 nm. The channel barrier thickness is t_B. Source and drain reservoirs have been doped with a molar fraction f, i.e. the ratio of the number of doping atoms over the total number of carbon atoms in the contacts.

The channel barrier consists of hexagonal Boron Nitride composites (h-BCN), in particular BN and BC_2N. Corresponding structures and energy dispersions are shown in Fig. 2.

The key parameters required for an accurate computation of transport through the barrier are those concerned with the graphene/h-BCN barrier height, especially electron affinity χ and the energy bandgap $E_{\rm gap}$. They are not available in the literature, and have therefore been computed on purpose through ab-initio simulations.

If the intrinsic Fermi level of graphene is considered as the referring potential (equal to zero) and $\chi_G = 4.248$ eV is graphene electron affinity, the barrier heights seen by electron and holes read

$$BC = \chi_G - \chi, \text{and} \quad (1)$$

$$BV = |\chi_G - \chi - E_{\rm gap}|, \quad (2)$$

respectively, as also sketched in Fig. 3.

The computed electron affinity χ and the energy gap $E_{\rm gap}$ are shown in Tab. III. In particular, within the adopted p_z tight-binding model, on-site energies for B and N atoms have been taken equal to BC and -BV, respectively: such assumption manages to reproduce the same $E_{\rm gap}$ and barrier height as in DFT calculations.

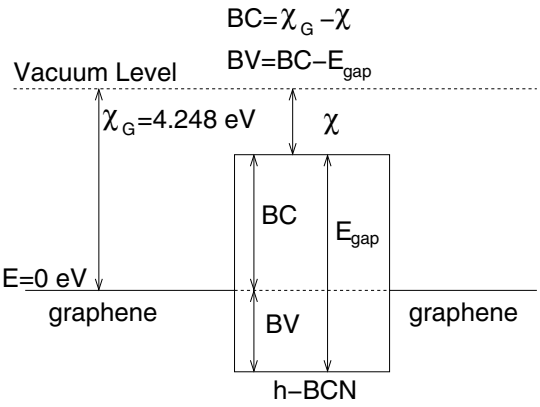

Fig. 3. Illustration of the band edge structure of the graphene/h-BCN/graphene system for a zero potential. BC (BV) represents the difference between the conduction (valence) band of the barrier and the intrinsic Fermi level in graphene.

Table I: Electron affinity (χ), energy gap (E_{gap}), barrier height for electrons (BC) and holes(BV) for two-dimensional composite materials h-BCN.

Material	χ (eV)	E_{gap} (eV)	BC (eV)	BV (eV)
BN	1.11	4.70	3.137	1.563
BC_2N	3.30	1.59	0.948	0.642

In Fig. 4, we show the transfer characteristics of a device with BC_2N barrier for different positions y_m of the middle of the barrier along the longitudinal direction, when applying a supply voltage V_{DD} equal to 0.6 V.

Since the barrier seen by holes is smaller than that seen by electrons in both BC_2N and BN, we have simulated pFETs. In the same picture, the transfer characteristics of a graphene FET is shown as reference. Whereas, as expected, the I_{on}/I_{off} ratio in graphene FET is smaller than 10, the gate voltage V_{GS} can modulate the drain current I_D in the BC_2N FET by four orders of magnitude, with no appreciable dependence on y_m. Metal gates show a good control over the channel barrier, as demonstrated by the sub-threshold swing (SS) close to 80 mV/dec.

In Fig. 5, the Local Density of States (LDOS) for a graphene FET and a graphene/BC_2N FET are shown for V_{GS}=-0.3 V: brighter colors correspond to higher LDOS values. In the graphene FET small values of LDOS are in correspondence of the intrinsic Fermi level along the device. As can be seen, the strong band-to-band tunneling component due to the zero bandgap leads to occupied states in the channel, degrading the electrostatic control of the gate over the channel barrier. In the BC_2N device instead, apart from the small LDOS in correspondence of the source and drain graphene reservoirs, a band-gap can be clearly seen in correspondence of the barrier, which in turn suppresses electron flowing from the drain.

As already noted above, despite the double-gate structure, SS is good but not ideal (60 mV/dec). This can be explained by the induced localized states in correspondence of the drain. As can be seen, a roughly triangular well is seen by electrons at the interface of the BN barrier and the doped drain reservoir. Such states are negatively charged, since holes tunnel through the almost transparent barrier towards the

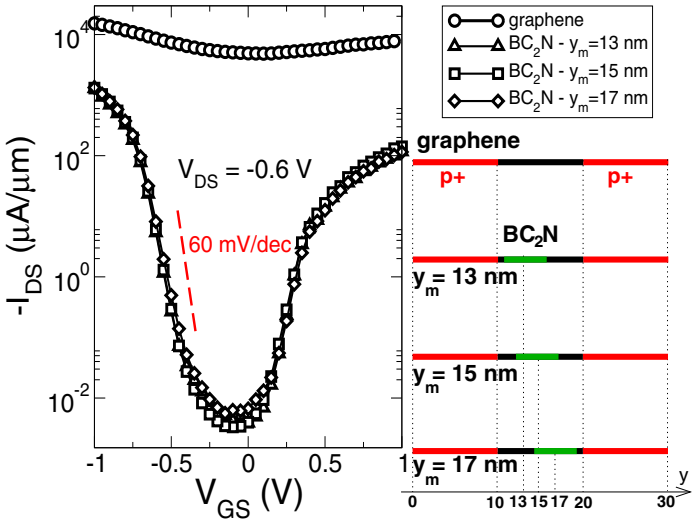

Fig. 4. Transfer characteristics for the BC_2N FET, considering different values of y_m, i.e. the coordinate of the middle of the barrier. t_B=5 nm.V_{DS}=-0.6 V and $f = 10^{-2}$.

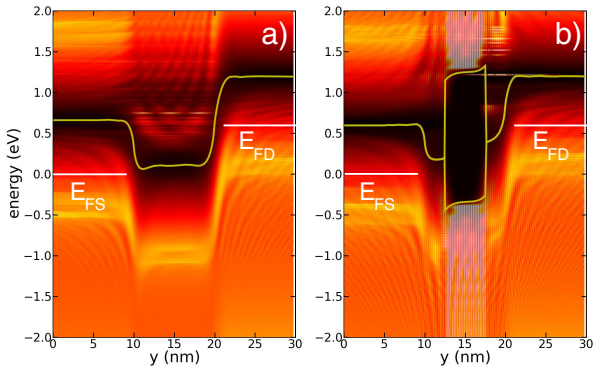

Fig. 5. Local Density of States (LDOS) for a) graphene and b) BC_2N p-MOS FET. The intrinsic Fermi level and the conduction and valence bands are depicted for the graphene and BC_2N device, respectively. E_{FS} (E_{FD}) is the Fermi level in the source (drain) reservoir. Brighter colors correspond to higher LDOS values.

drain, leaving an electron in the channel. In order to reduce such charge, thicker barriers can be considered. Attention must however be paid in order not put the barrier in direct contact with the reservoirs, since problems may arise due the formation of a Schottky-like contact, which could further reduce the gate control over the channel barrier.

In Fig. 6a, we show the transfer characteristics for both BN and BC_2N devices. Due to the large BN barrier height, BN devices show larger threshold voltage, and smaller I_{on}, but SS similar to those obtained in BC_2N device. The transfer characteristics of a BC_2N FET for different values of t_B are shown in Fig 6b. As can be seen, as long as the barrier thickness is reduced, barrier becomes more transparent and the subthreshold behavior is degraded, so that transfer characteristics come closer to those of a graphene FET.

In Table II, we show the main figures of merit of FET performance. In particular the intrinsic delay time τ and the power-delay product PDP are defined as:

$$\tau = \frac{C_G V_{DD}}{I_{on}} \tag{3}$$

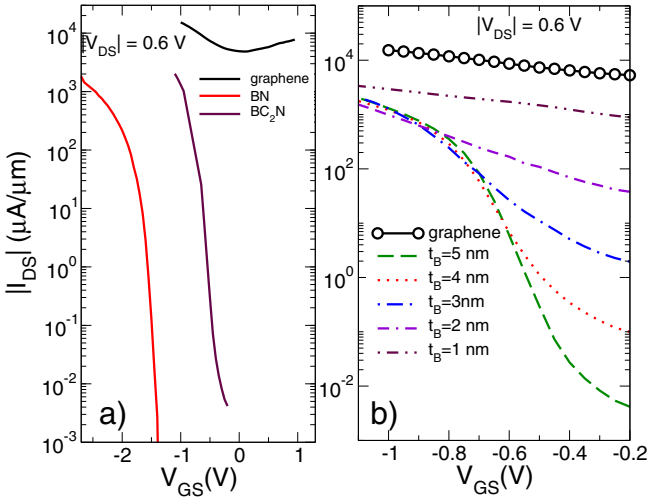

Fig. 6. a) Transfer characteristics for the different barrier materials. All the considered devices are p-type. Molar fraction $f = 10^{-2}$ for BC_2N, $f = 5 \times 10^{-2}$ for BN. t_B=5 nm. b) Transfer characteristics for the BC_2N device for different barrier thicknesses t_B and y_m=15 nm. In both pictures, graphene transfer characteristic is shown as a reference.

Table II: Channel length (L), $|I_{off}|$, $|I_{on}|$, I_{on}/I_{off} ratio, subthreshold swing (SS), Power Delay product (PDP) and intrinsic device speed (τ) for the different simulated devices.

Material	L (nm)	$\|I_{off}\|$ ($\mu A/\mu m$)	$\|I_{on}\|$ ($\mu A/\mu m$)	I_{on}/I_{off}	SS (mV/dec)	PDP (J/m)	τ (ps)
BC_2N	10	0.1	1736	17360	80	1.01×10^{-10}	0.097
BC_2N	7	0.1	1600	16000	83	7.84×10^{-11}	0.0817
BN	10	0.1	491	4910	70	2.82×10^{-10}	0.96

$$PDP = V_{DD} I_{on} \tau, \tag{4}$$

where C_G is the total gate capacitance, computed as the derivative of the the charge in the whole device for $V_{DS} = V_{DD}$, with respect to V_{GS}.

Except the BN device, BC_2N FETs show I_{on}/I_{off} larger than 10^4, meeting ITRS requirements.

In order to investigate the RF performance, we have computed with a quasi-static model the intrinsic cut-off frequency f_T, which reads

$$f_T = \frac{g_m}{2\pi C_G}, \tag{5}$$

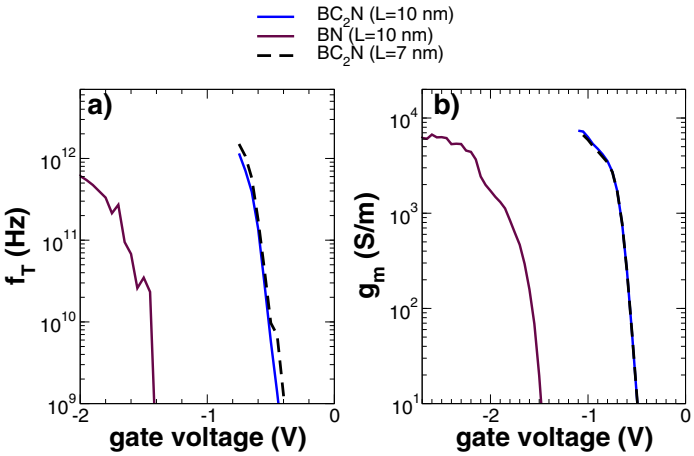

Fig. 7. a) Cut-off frequency defined as $f_T = g_m/2\pi C_G$, where g_m is the device transconductance and C_G the gate capacitance, as a function of V_{GS} for the different h-BCN barriers. b) g_m as a function of V_{GS} for the different h-BCN barriers.

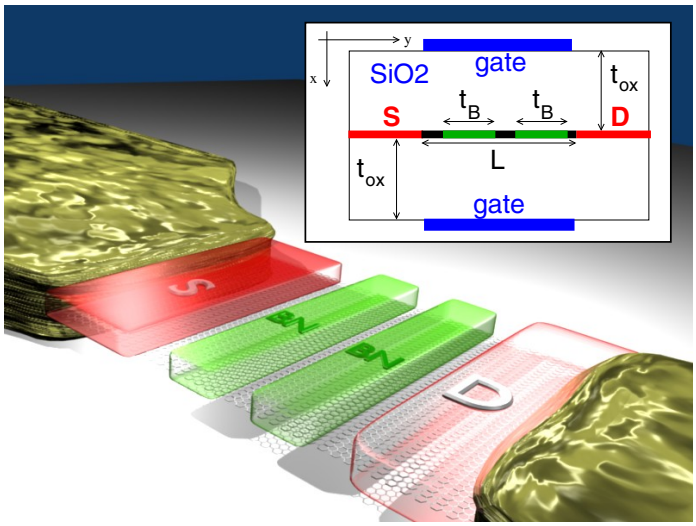

Fig. 8. Sketch of the RT device with double BN barriers in the channel. In the inset, longitudinal cross-section of the device is shown.

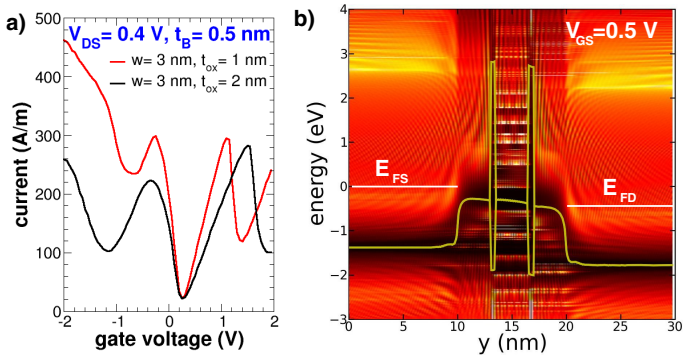

Fig. 9. a) I_{DS} *vs* V_{GS} for a device with a BN double barrier with the same t_B and w=3 nm. Two different values of t_B have been considered. b) LDOS for V_{GS}=0.5 V.

where g_m is the transconductance, defined as the derivative of I_D with respect to V_{GS}.

Results are shown in Fig. 7a, where f_T reaches the THz range. In Fig. 7b the transconductance g_m is shown as a function of the gate voltage.

We mentioned nanodevices in Flatland in the title because the graphene/BCN material system allows to obtain, in a truly two-dimensional fashion, several device concepts. An interesting example is the resonant tunneling (RT) FET, where two t_B-thick BN stripes are considered in the channel, separated by a graphene region w-nm large (Fig. 8).

In this case the two barriers form a Fabry-Perot resonator for charge carriers that can be modulated in energy through the gate voltage. This can introduce a negative transconductance region as shown in Fig. 9a. As can be seen, the thinner the field oxide, the larger the gate control over the channel barrier, and the steeper the regions where negative differential transconductance appears.

In Fig. 9b, the LDOS is shown for V_{GS}=0.5 V. As can be seen, localized states appear in the middle of the channel, and are shifted upwards and downwards by the gate voltage. Whenever a resonant states aligns with the Fermi level of the source, a peak appears in the I_D-V_{GS} characteristics.

The real advantage of the proposed RT-FET over previous different proposals of resonant tunneling transistors, such as those based on III-V material systems [11], is the extremely good electrostatic control of the devices, unachievable with bipolar operation.

IV. Final Remarks

We have shown that hybridized graphene with intercalated carbon and h-BCN represent an exceptional platform for exploring truly two-dimensional nanoelectronics. The possibility to engineer the electronic properties of the channel with h-BCN allows to obtain high $I_{\rm on}/I_{\rm off}$ graphene-based FETs. When considering two-barriers instead of one, negative differential transconductance can be obtained, so that resonant tunneling FET, interesting for beyond CMOS applications, can be realized.

V. Acknowledgments

This work was supported in part by the EC 7FP through the Network of Excellence NANOSIL (Contract 216171), by the Project GRAND (Contract 215752), by the European Science Foundation EUROCORES Programme Fundamentals of Nanoelectronics, through funding from the CNR (awarded to IEEIIT-PISA) and the EC 6FP, under Project Dewint (Contract ERASCT- 2003-980409), and by the MIUR-PRIN "Modeling and simulation of graphene nanoribbon FETs for high-performance and low-power logic applications" project (Prot. 2008S2CLJ9).

References

[1] L. Ci et al.,"Atomic layers of hybridized boron nitride and graphene domains", *Nature Materials*, Vol. 9, p. 430, 2010.
[2] M. C. Lemme et al., "A graphene field-effect device", IEEE Electr. Dev. Lett., Vol. 28, p. 282, 2007.
[3] Ph. Avouris et al., "Carbon-based electronics", Nat. Nanotech., Vol. 2, p. 605, 2007.
[4] P. Giannozzi et al., "Quantum ESPRESSO: a modular and open-source software project for quantum simulations of materials", *J. Phys.: Condens. Matter*, Vol. 21, p. 395502, 2009.
[5] url: http://www.nanohub.org.tools/vides
[6] G. Fiori et al., "On the possibility of tunable-gap bilayer graphene FET", *Electron Dev. Lett.*, Vol. 30, p. 261, 2009.
[7] G. Fiori et al., "Ultralow-Voltage Bilayer graphene tunnel FET", *IEEE Electr. Dev. Lett.*, Vol. 30, pp.1096-1098, 2009.
[8] J. Zhu et al., "Interpolation of aotmically thin hexagonal boron nitride and graphene: electronic structure and thermodynamic stability in terms of all-carbon conjugated paths and aromatic hexagons", *J. Phys. Chem.C*, Vol. 115, p. 10264, 2011.
[9] M. Wimmer, *PhD Thesis*, 2009.
[10] M. P. L. Sancho, J. M. L. Sancho, and J. Rubio, "Highly convergent schemes for the calculation of bulk and surface green function" *J. Phys. F, Met. Phys.*, Vol. 15, p. 851, 1985.
[11] F. Capasso et al. *IEDM Tech. Dig.*, p. 282, 1986.